Multilevel Algorithms

Pushan Majumdar

(Department of Theoretical Physics, Indian Association for the Cultivation of Science, Jadavpur, Kolkata)

Observables in non-Abelian gauge theories

$$\langle \mathcal{O} \rangle = Z^{-1} \int \mathcal{D}A\mathcal{D}\bar{\psi}\mathcal{D}\psi \; \mathcal{O} \; e^{-S} \tag{1}$$

where $S = \bar{\psi} \not{D}(A) \psi + F^2(A)$.

Even if we drop the fermions, S is quartic in A. Functional integral cannot be done analytically.

Two options :

1) Expand e^{-S} as a series in g.

2) Estimate the integral numerically.

(1) works for small values of g and leads to perturbative QCD.

(2) is fully non-perturbative, but requires a discretization for implementation. This leads to lattice gauge theory.

Wilson's LGT : Discretization maintaining gauge invariance.

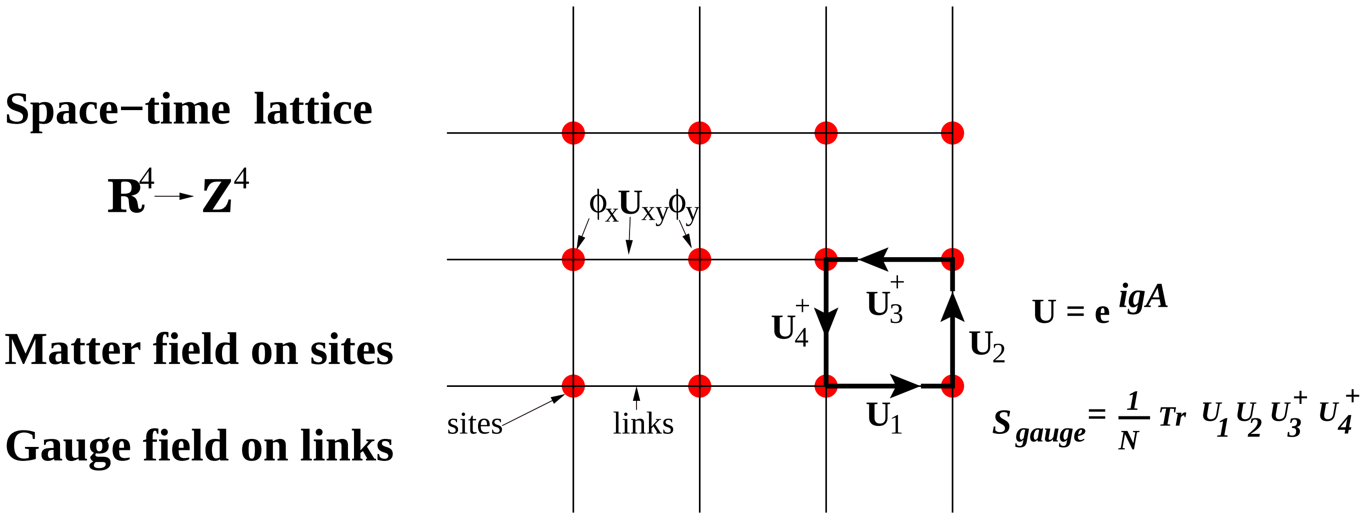

finite lattice spacing : UV cut off   finite lattice size : IR cut off

Periodic boundary conditions to avoid end effects $\Rightarrow \mathbf{T}^4$ topology.

Finally one must extrapolate to zero lattice spacing.

ACTION : $S(\mathit{Fields(x)}\ ,\ \mathit{bare\ couplings})$

Finite Lattice (Finite degrees of freedom) **:** N^4 **points**

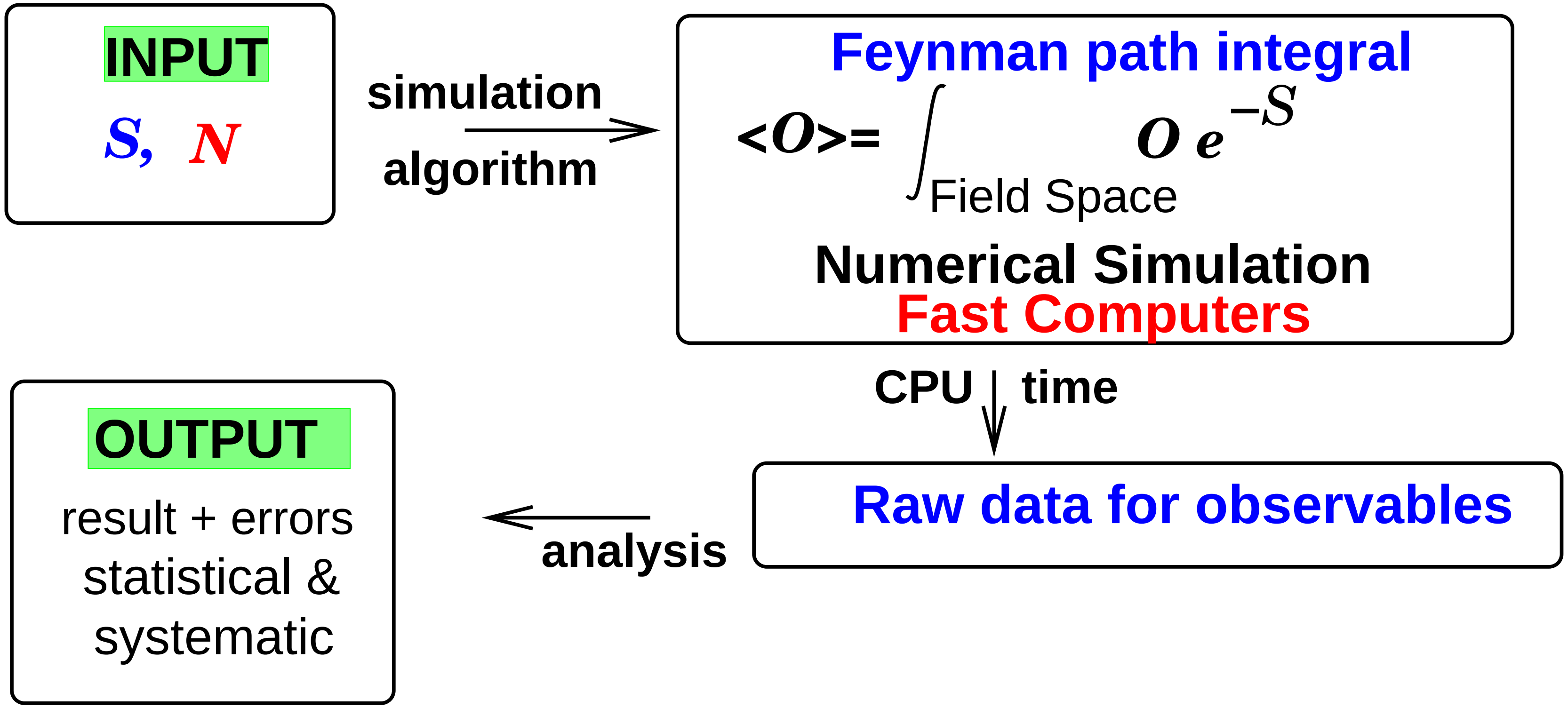

dimension of the integral : $4 \times N^4$

domain of integration : manifold of the group SU(3)

Not possible to do exactly – use sampling techniques

Heat-Bath update for pure SU(2) lattice gauge theory

Change in action due to changing a single link.
Probability of a link U is given by
$P(U) \propto \exp(\frac{1}{2}\beta \, \mathrm{Tr}\, (U \times \text{sum of staples}))$
where $dU = \frac{1}{2\pi^2}\,\delta(s^2 - 1)\, d^4 s$ is the invariant Haar measure of the group $SU(2)$.

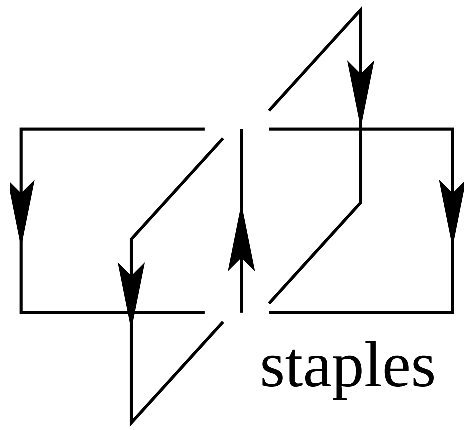

If $U \in SU(2)$ then $U = s_0 + i s_i \sigma_i$ where σ_i are Pauli matrices.
Using this parametrization it is possible to generate U's with the required probability.
As if the link to be updated is brought in contact to a heat - bath.

Unlike Metropolis the acceptance probability in heat-bath algorithms is one.

Confinement on the lattice

- Mechanism of Confinement : On the lattice there is evidence of flux tube formation.

- Conjecture : Flux tube $\equiv$ bosonic string.

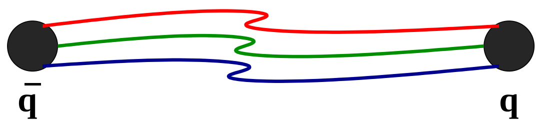

- Effective theories for flux tubes (hadronic strings) .

- Zero-mass fluctuations of the string $\rightarrow$ power corrections to static quark potential
  Coefficient of leading correction: Universal & One loop exact: Lüscher term - value $= -\frac{(d-2)\pi}{24}$

Observables for pure Yang-Mills theories on the lattice

- Polyakov loop correlators:
  Accurate ground state energy.

$$\langle P^\dagger P(r)\rangle = \sum_{i=0}^{\infty} b_i \ \mathrm{exp}[-E_i(r)N_t]$$

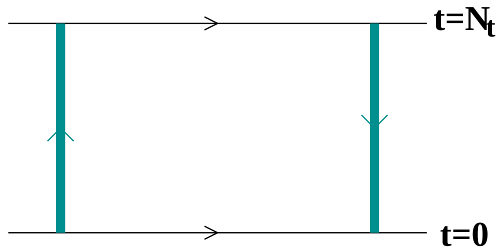

Polyakov Loop correlator

- Wilson loops :
  Suitable for excited states

$$W(r,\Delta T) = \sum_\alpha \beta_i^\alpha \beta_j^\alpha e^{-E_\alpha(r)\Delta T}$$

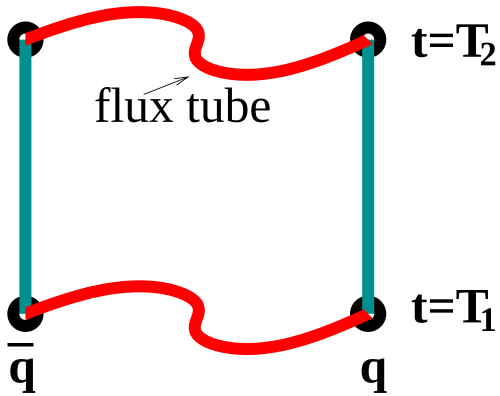

Wilson Loop

- The string pictures holds at large $r \Rightarrow$ large loops.

- Note that $W(r, \Delta T) \propto \exp(-r\Delta T)$

- Since we need large r, we must either work with small ΔT, or have the means to extract exponentially suppressed signals from the noise.

- 1st alternative requires using asymmetric lattices and a very large number of basis states.

- Advances in algorithms (e.g. multilevel schemes) * and computing power now allow for exponential error reduction and reliable extraction of expectation values of large Wilson loops.

*These are special algorithms which work only for pure Yang-Mills theories

Error reduction by multihit

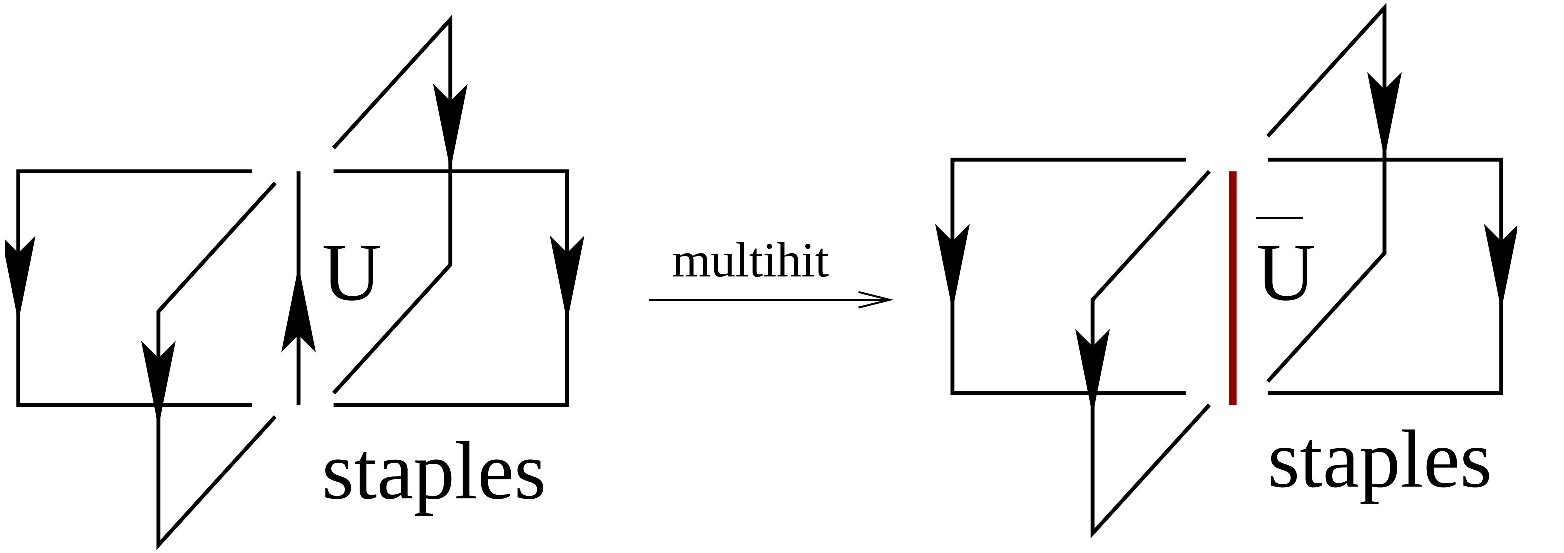

Replacing the link U by the averaged link $\bar{U}$ gives a smaller variance for the final observable.

$$\bar{U} \equiv \frac{\int dU \, \exp[(\beta/N) \mathrm{Re\,Tr}(US)] U}{\int dU \, \exp[(\beta/N) \mathrm{Re\,Tr}(US)]}$$

While computing the expectation value of an observable, more than one link can be simultaneously replaced by their averages as long as no two such links are on the same plaquette.

For $SU(2)$, the analytic expression for $\bar{U}$ is given by

$$\bar{U} = KS^{-1}\frac{I_2(\beta K)}{I_1(\beta K)} \qquad \text{where} \quad K = |\det S|^{\frac{1}{2}}.$$

For higher N's it is more convenient to estimate $\bar{U}$ by Monte Carlo integration.

For SU(3) a semi-analytic method due to de Forcand & Roiesnel is much more efficient than Monte Carlo integration.

The multilevel algorithm can be thought of as a generalization of the multihit procedure.

Algorithm - Ground State

- $a \otimes b =$ T1(2,2,2,2)

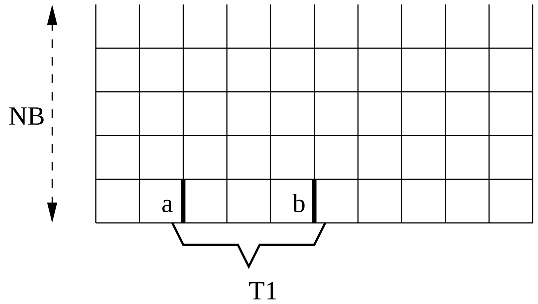

- $(\mathrm{T1})_{ijkl}(\mathrm{T2})_{jmln}{=}(\mathrm{Tp1})_{imkn}$ Averaging is carried out for Tp1.

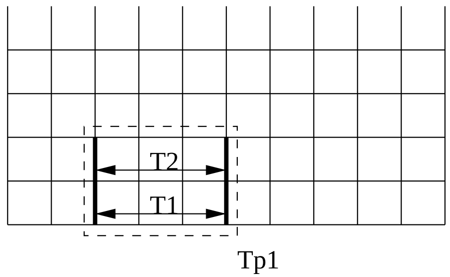

- The averaged Tp's are multiplied together to form the averaged propagator Tf.

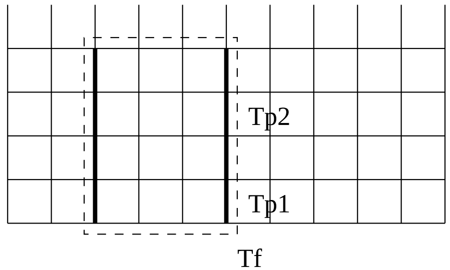

- L1, L2 & Tf are multiplied together to produce the Wilson loop.

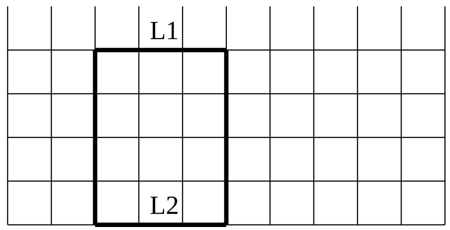

Important parameters of the algorithm : time slice thickness - Tp1 & the number of sublattice updates $iupd$.

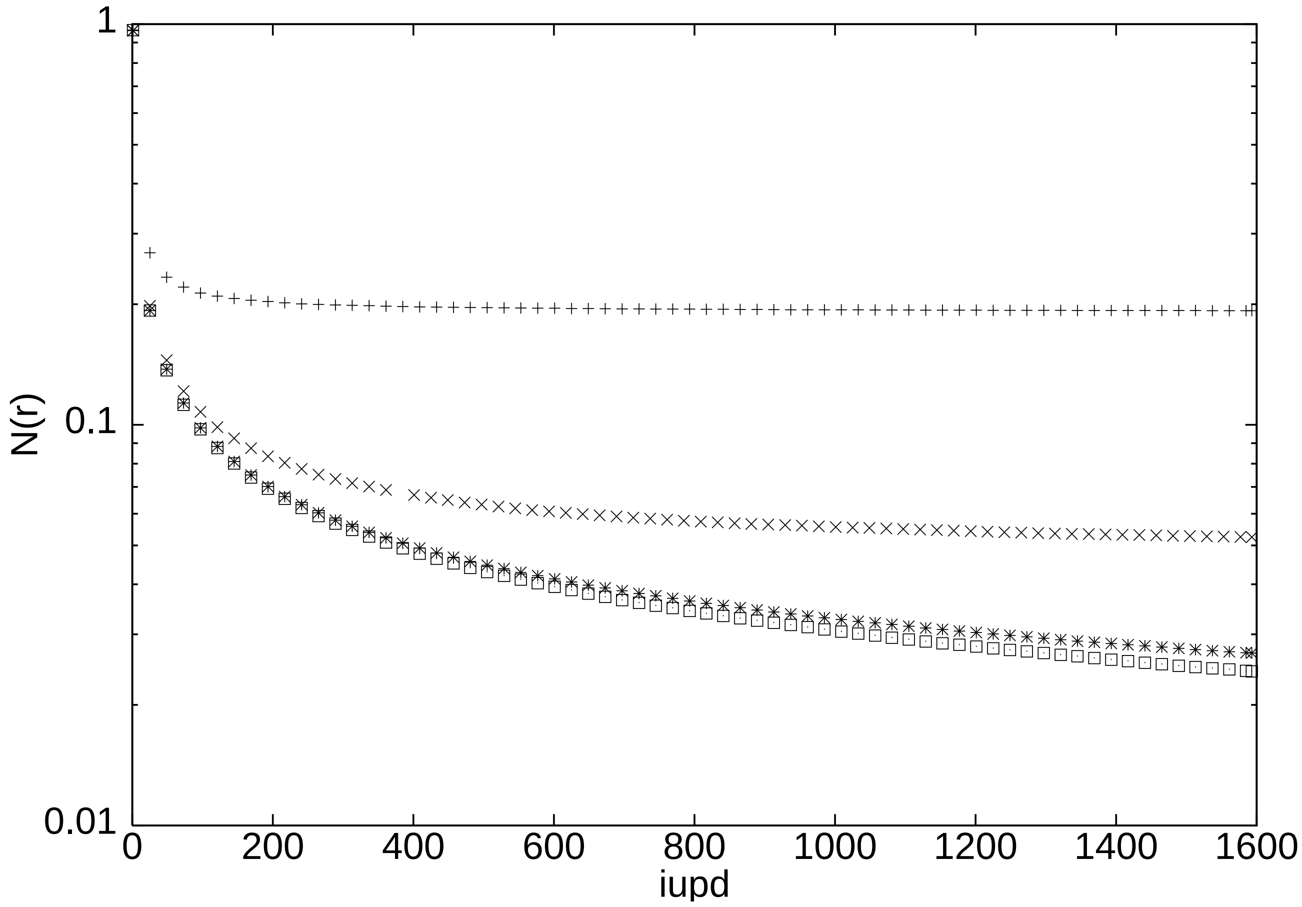

2-link norm vs $iupd$ for r=2,4,6 and 8 at $\beta = 3$ (3-d SU(2) LGT).

Error on $\langle W(12,12)\rangle$at $\beta = 5$ with iupd.

iupd	meas	average	error	time
100	100	1.47×10^{-8}	1.53×10^{-8}	59m
200	100	6.13×10^{-9}	4.6×10^{-9}	115m
400	100	1.11×10^{-8}	2.8×10^{-9}	229m
800	100	9.39×10^{-9}	2.1×10^{-9}	454m
1600	100	1.17×10^{-8}	1.81×10^{-9}	899m

Ratio of error between iupd of 100 & 1600 is 8.45.

Error of sample mean $\propto \frac{1}{\sqrt{n}}$ where n is the number of measurements.

Therefore ratio of times should have been $8.45^2 = 71.45$ but is only 15.2.

- Potential between static $q\bar{q}$ pair: (series in r^{-n})

$$V(r) \sim \sigma r + \widehat{V} - c/r + \cdots$$

Arvis : Ground state of Nambu-Goto string :

$$V_{\mathrm{Arvis}} = \sigma r \left(1 - \frac{(d-2)\pi}{12\sigma r^2}\right)^{1/2}$$

Potential turns complex at $r = r_c$ (tachyons).

We look at the first and a scaled second derivative of $V(r)$.

$$f(\bar{r}) \;=\; V(r) - V(r-1) \qquad \text{with} \qquad \bar{r} = r + \frac{a}{2} + \mathcal{O}(a^2)$$

$$c(\tilde{r}) \;=\; \frac{\tilde{r}^3}{2}[V(r+1) + V(r-1) - 2V(r)] \quad \text{with} \quad \tilde{r} = r + \mathcal{O}(a^2)$$

$\bar{r}$ & $\tilde{r}$ reduce lattice artefacts.

String predictions (d=3)

L.O. $f(r) = \sigma + \left(\frac{\pi}{24}\right)\frac{1}{r^2}$ $\qquad c(r) = -\frac{\pi}{24}$

N.L.O. $f(r) = \sigma + \left(\frac{\pi}{24}\right)\frac{1}{r^2} + \left(\frac{\pi}{24}\right)^2 \frac{3}{2\sigma r^4}$ $\qquad c(r) = -\frac{\pi}{24}\left(1 + \frac{\pi}{8\sigma r^2}\right)$

Arvis $f(r) = \sigma\left(1 - \frac{\pi}{12\sigma r^2}\right)^{-1/2}$ $\qquad c(r) = -\frac{\pi}{24}\left(1 - \frac{\pi}{12\sigma r^2}\right)^{-\frac{3}{2}}.$

Perturbation theory

$$V_{\text{pert}}(r) = \sigma_{\text{pert}} r + \frac{g^2 C_F}{2\pi} \ln g^2 r + (\text{higher order terms}) \qquad (2)$$

$\sigma_{\text{pert}} = \frac{7g^4 C_F C_A}{64\pi}$ with $C_F = 3/4$ and $C_A = 2$.

β	r_0/a	r values	lattice	iupd	# of meas.
5.0	3.9536(3)	$2-8$	36^3	16000	1600
(ts=2)		$7-9$	40^3	32000	3200
		$8-12$	48^3	48000	20800
7.5	6.2875(10)	$4-8$	48^3	8000	1100
(ts=4)		$7-12$	64^3	18000	1100
		$11-16$	64^3	36000	7200
		$13-17$	64^3	48000	6700
10.0	8.6022(8)	$2-7$	48^3	16000	2850
(ts=4)		$6-9$	48^3	16000	200
		$8-14$	84^3	24000	1100
		$13-19$	84^3	36000	2250
12.5	10.916(3)	$2-9$	48^3	16000	2700
(ts=6)		$8-14$	72^3	24000	1150

$r_0^2 f(r)$ **vs** r/r_0

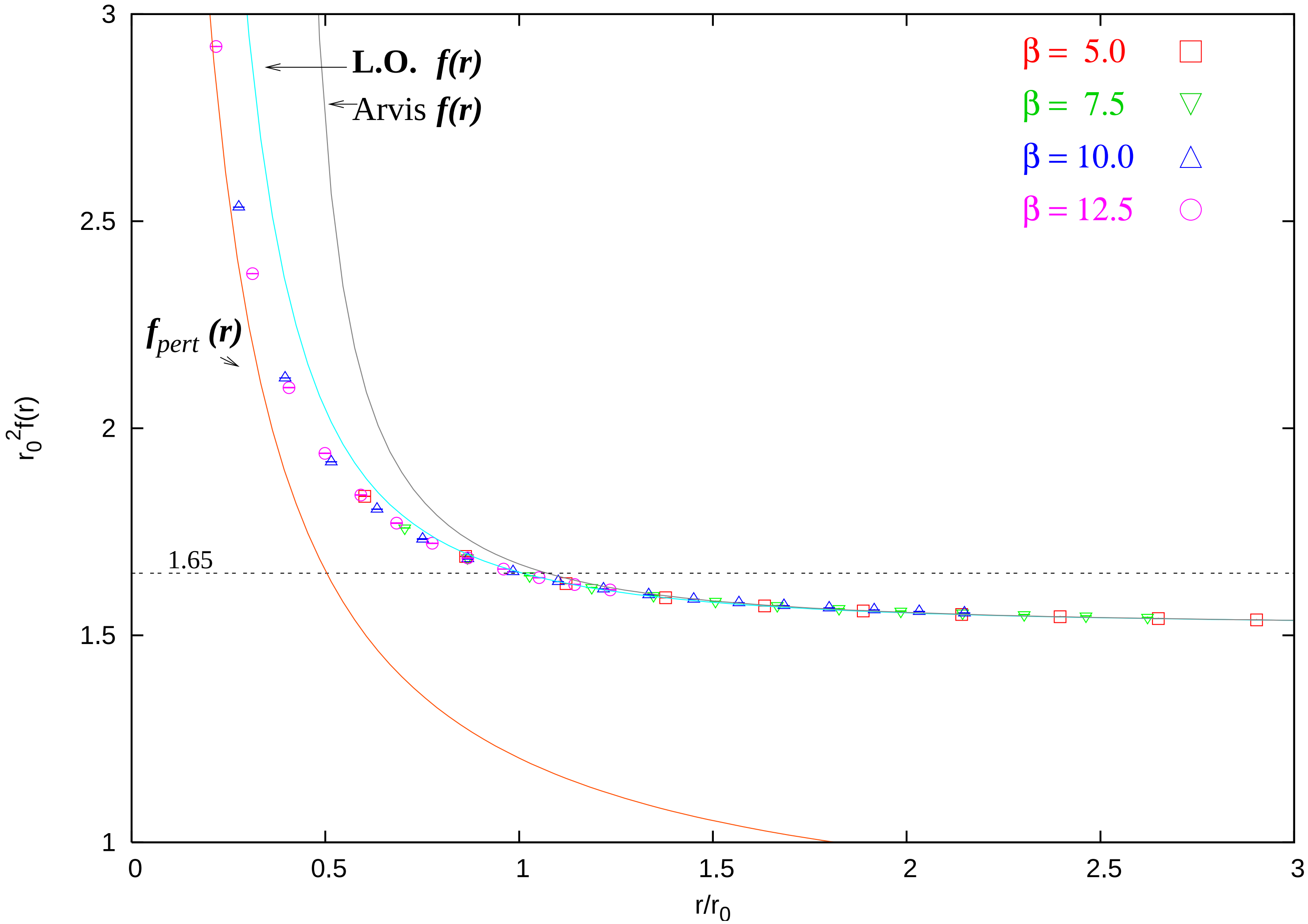

$f_{\text{pert}}(r)$: 1-loop perturbation theory.
Dotted line : $r_0^2 f(r) = 1.65$, locates the Sommer scale. (3-d SU(2) LGT)

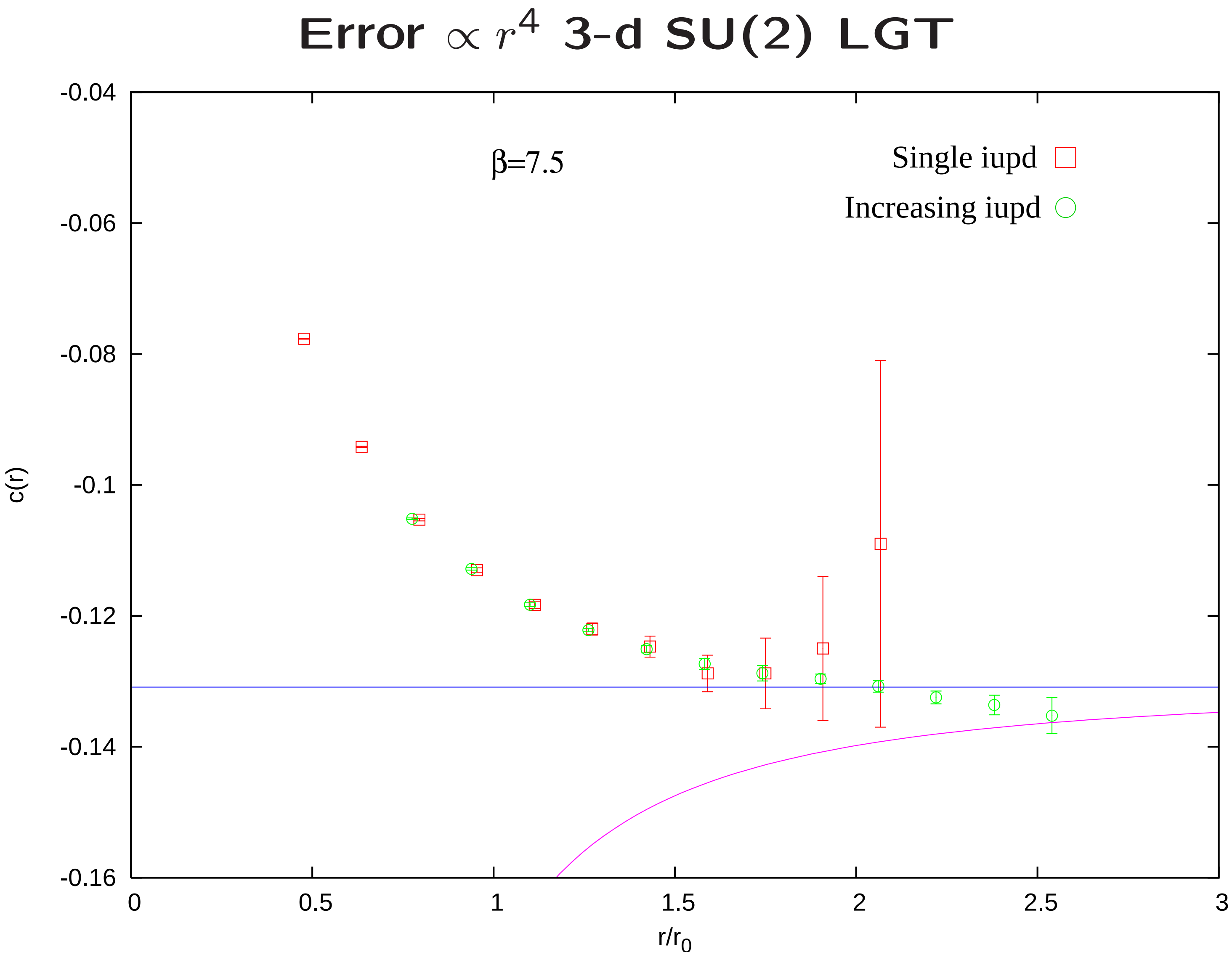

Error ∝ r^4 3-d SU(2) LGT
β=7.5
Single iupd
Increasing iupd
c(r)
r/r_0
-0.04
-0.06
-0.08
-0.1
-0.12
-0.14
-0.16
0
0.5
1
1.5
2
2.5
3

Interpolating curves

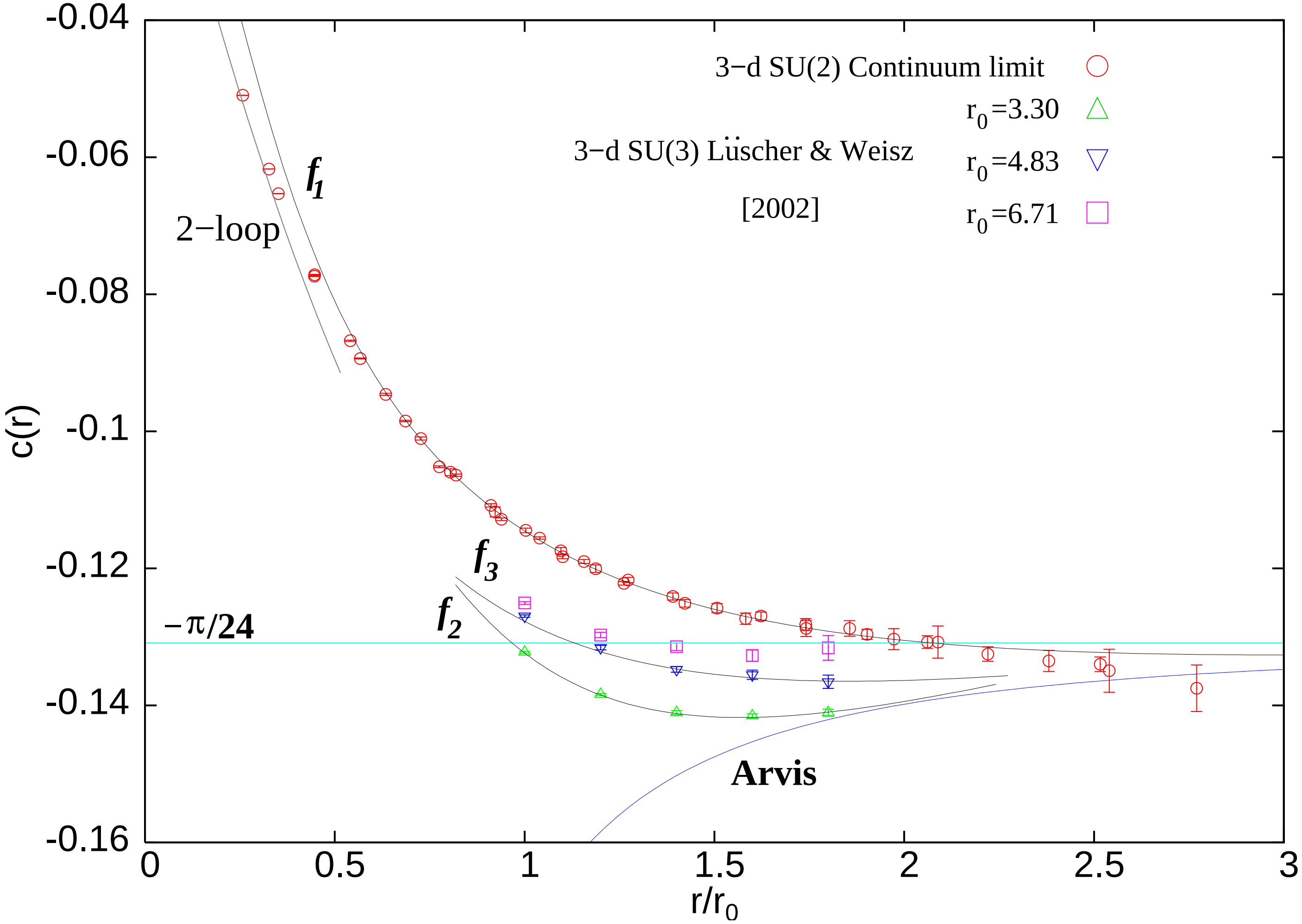

Non-monotonicity of the approach to the Lüscher term.

Excited states of the flux tube

Behaviour under charge conjugation and parity – **CP**

P: Reflect in $q\bar{q}$ axis : $x(\kappa) \longrightarrow -x(\kappa)$

C: Interchange q and $\bar{q}$: $x(\kappa) \longrightarrow x(r-\kappa)$

Combinations $\Leftrightarrow$ symmetry channels.

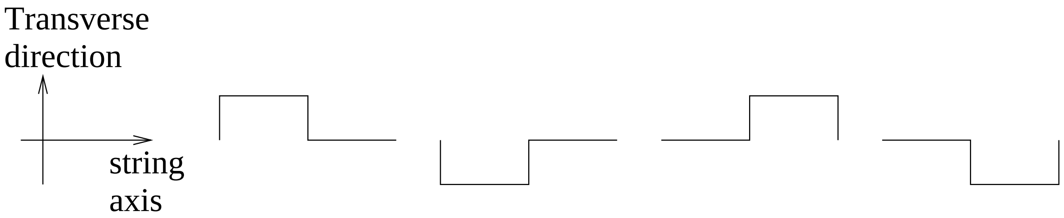

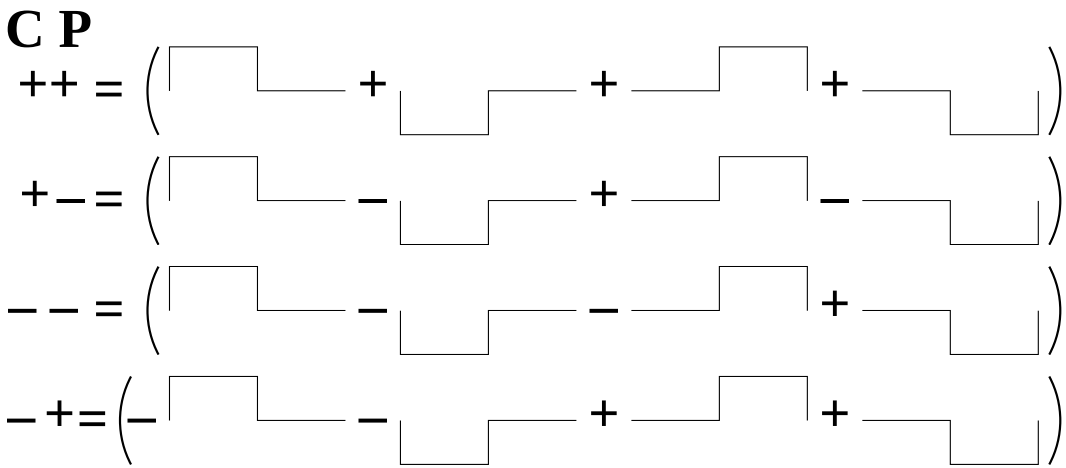

Algorithm - Excited states

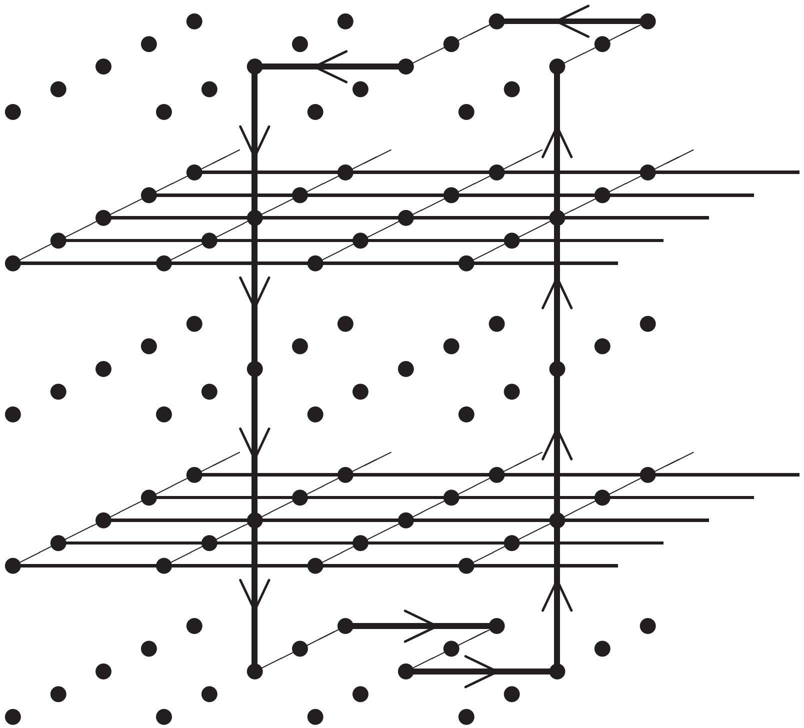

A wilson-loop with different sources at the ends, that lie in the middle of the time-slices. The slices with the solid lines are the time slices with fixed lines during the sublattice updates.

r	W_1 New	W_1 Old	W_2 New	W_2 Old	W_3 New	W_3 Old
4	0.44	0.15	2.7	7.0	9.2	100
5	0.63	0.21	2.7	8.3	8.6	100
6	0.86	0.28	2.7	4.5	8.8	100
7	1.1	0.35	2.9	7.3	8.8	100
8	1.4	0.45	3.1	5.5	9.5	100
9	1.7	0.56	3.6	10	11	100
10	2.1	0.74	4.2	11	14	100
11	2.7	1.0	5.8	27	22	100
12	3.5	1.7	8.6	88	44	100

Percentage errors for Wilson loops for energies E_1, E_2 and E_3.
$\beta = 5$, $T = 8$ with r varying between $4 - 8$. Time $\approx$ 1100 mins.

Old method: 730 mesurements with no source averaging.

New method: 50 mesurements with 12000 updates for source averaging.

2-link averaging was same for both methods.

Energy of the string excited states

$$\text{L.O.} \quad E_n = \sigma r + \mu + \frac{\pi}{r}(n - \frac{d-2}{24})$$

$$\text{N.L.O} \quad E_n = \sigma r + \mu + \frac{\pi}{r}(n - \frac{d-2}{24}) - \frac{\pi^2}{2\sigma r^3}(n - \frac{d-2}{24})^2$$

$$\text{Arvis} \quad E_n = \sigma r(1 + \frac{2\pi}{\sigma r^2}(n - \frac{d-2}{24}))^{1/2}$$

We will look mostly at the energy difference $E_n - E_m$.

Correction factors

$$\lambda(T) = \alpha_1 e^{-ET}\left(1 + \frac{\alpha_2}{\alpha_1} e^{-\delta T}\right)$$

$$-\frac{1}{T_2 - T_1} \log \frac{\lambda(T_2)}{\lambda(T_1)} = \bar{E} + \frac{1}{T_2 - T_1}\left[\frac{\alpha_2}{\alpha_1} e^{-\delta T_1}\left(1 - e^{-\delta(T_2 - T_1)}\right)\right].$$

Excited state energies at $\beta = 5$ and $\beta = 7.5$.

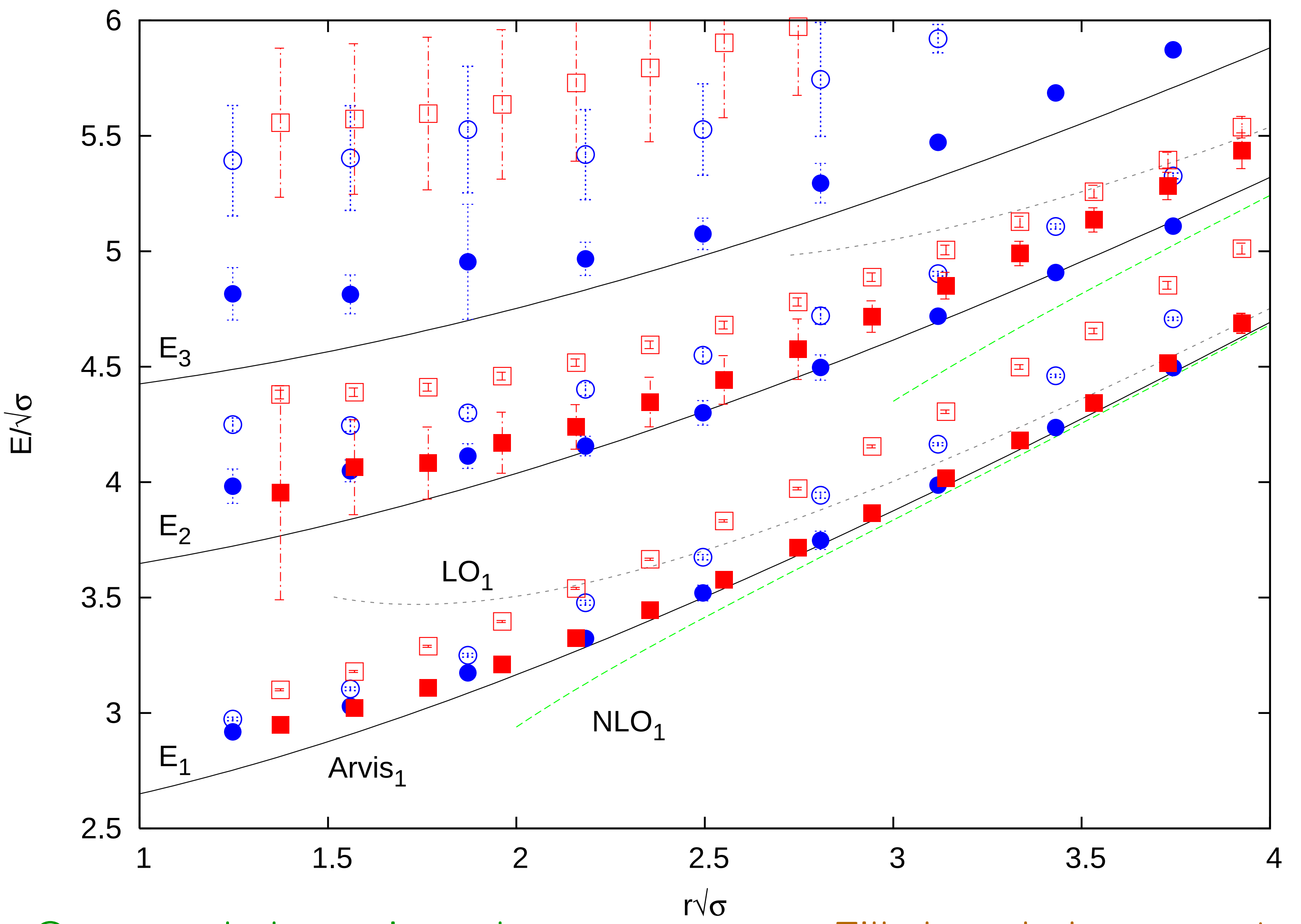

Open symbols : naive values

Filled symbols : corrected values.

Energy difference at $\beta = 5$ and $\beta = 7.5$.

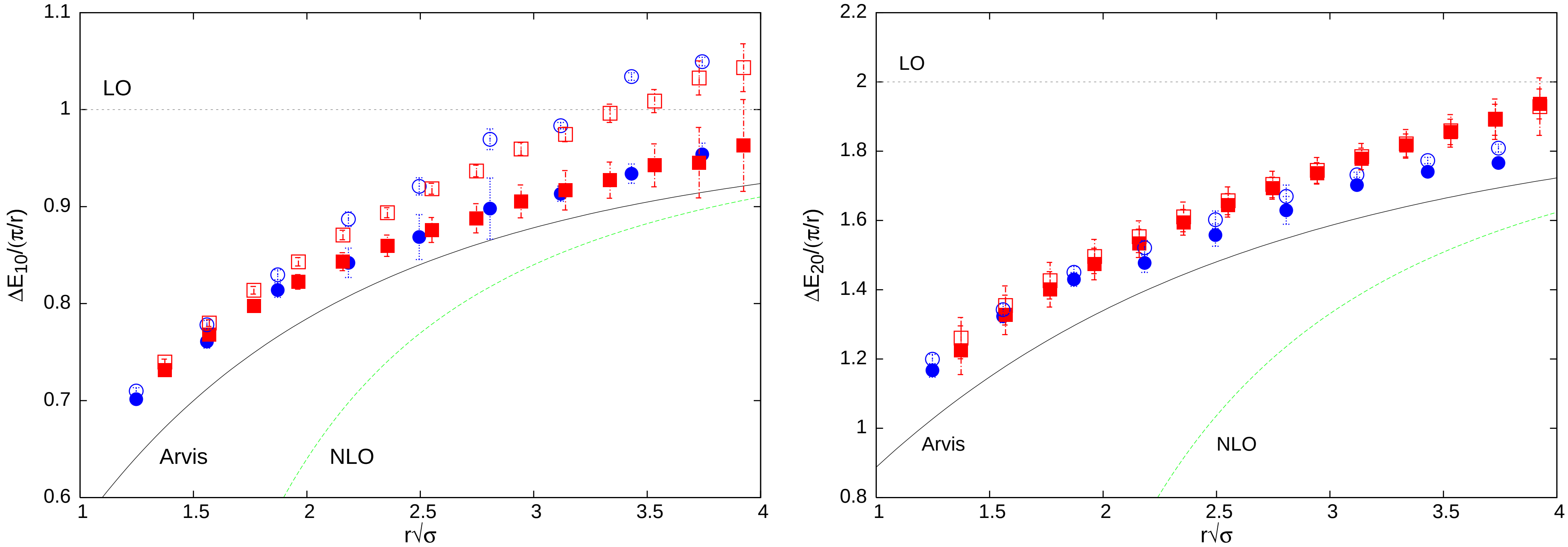

The distance corresponding to $r\sqrt{\sigma} = 4$ is about 1.6 fermi.

At $r\sqrt{\sigma} = 4$ and ΔE_{10} the difference between the **L.O.** and Arvis curves are $< 10\%$. For ΔE_{20} the difference is about 20%.

For ΔE_{20} at $\beta = 7.5$, the corrections are still not fully under control.

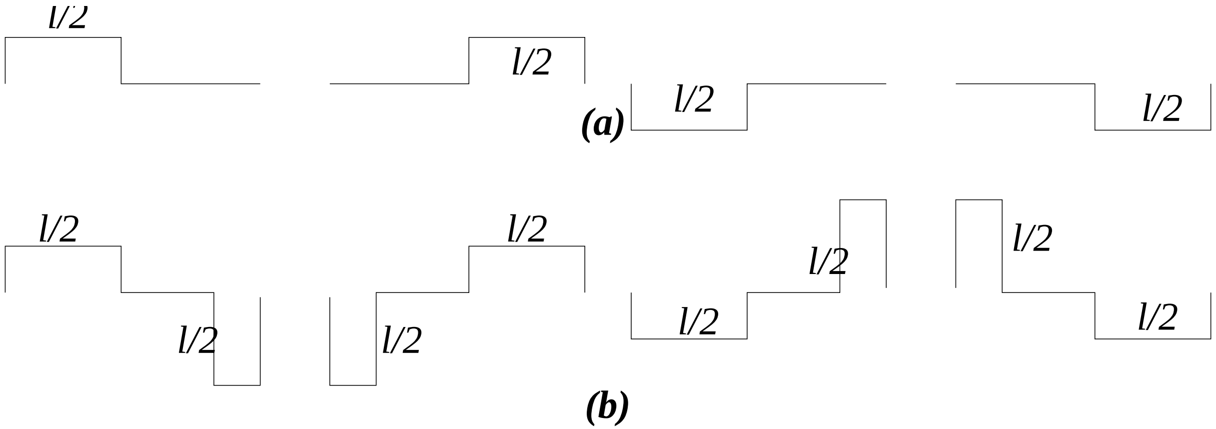

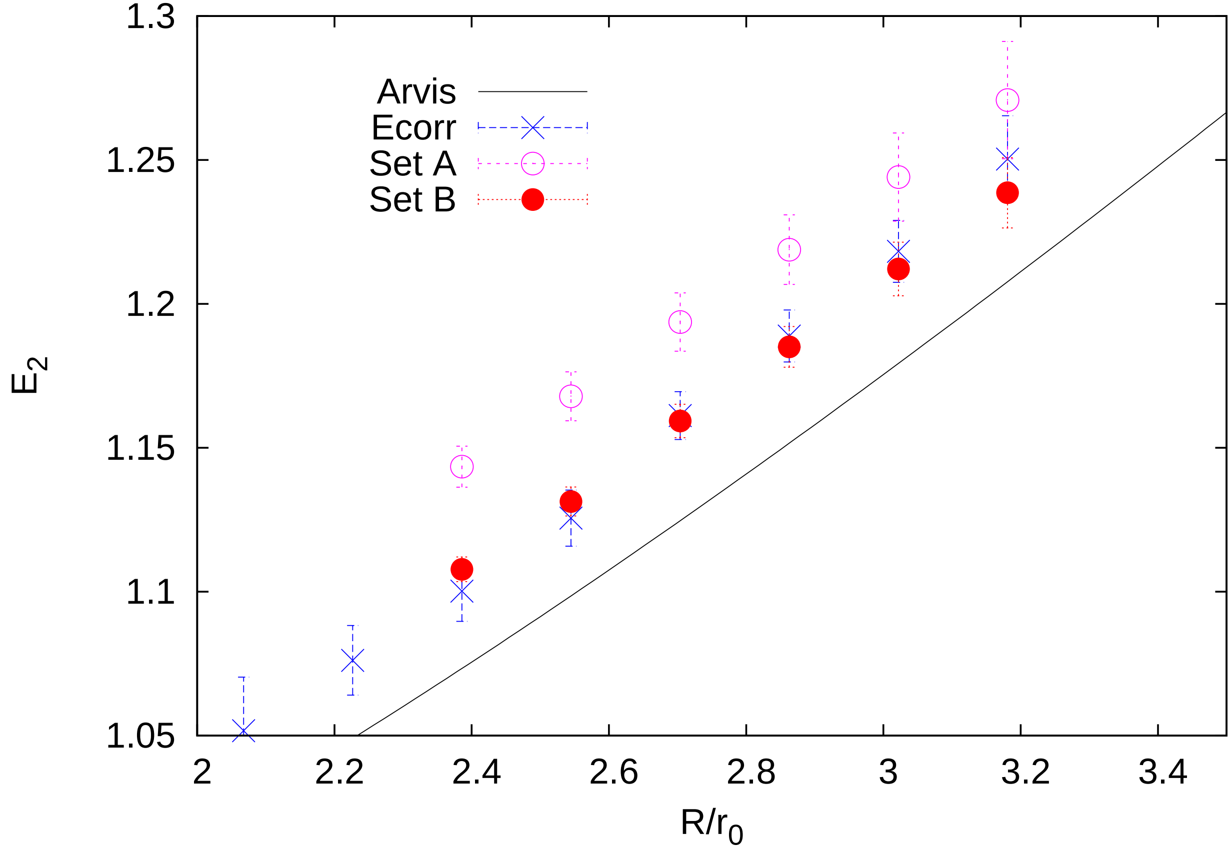

E_2 requires a better "wave function" as we approach continuum limit.

Used source (b) to couple strongly to E_2.

Plot shows E_2 values using source (a) and (b).

Values using (b) coincide with the corrected values from (a), but have lower error bars.

Glueball correlator

- $\langle C(t_1, t_0)\rangle_{\text{conn}} = \langle \mathcal{O}(t_1)\mathcal{O}(t_0)\rangle - \langle \mathcal{O}(t_1)\rangle\langle \mathcal{O}(t_0)\rangle$

$$\mathcal{O} \equiv \mathbf{Re}(\sum_{ij=1,2,3} P_{ij}) : \text{Scalar glueball}$$

$$\mathcal{O} \equiv \mathbf{Im}(P_{ij}) : \text{Axial} - \text{vector}.$$

P_{ij} : Plaquette in the ij plane.

$$\text{State with momentum } \vec{k} : \sum_{\vec{x}} \mathcal{O}(\vec{x}) e^{i\vec{k}\cdot\vec{x}}$$

- Time dependence of correlator :

$$\langle C(t_1, t_0)\rangle_{\text{conn}} \approx \alpha \left[e^{-m(t_1 - t_0)} + e^{-m(N_t - (t_1 - t_0))} \right]$$

- Scalar channel : non-zero VEV.
  Derivative to suit the multi-level algorithm.

$$\partial_{t_1}\partial^*_{t_0}\langle C(t_1,t_0)\rangle \approx -\alpha\left[e^{-m(t_1-t_0)}(1-e^{-m})^2 + e^{-m(N_t-(t_1-t_0))}(e^m-1)^2\right].$$

- In scalar channel (only $\vec{k}=0$) both $\partial_t\partial^*_{t_0}\langle C(t,t_0)\rangle$ and $\partial^*_t\partial_{t_0}\langle C(t,t_0)\rangle$ where

$$\partial_t\partial^*_{t_0}\langle C(t,t_0)\rangle = \langle\sum_{ij}\left[P_{ij}(t+1)-P_{ij}(t)\right]\sum_{ij}\left[P_{ij}(t_0)-P_{ij}(t_0-1)\right]\rangle \tag{3}$$

- Axial-vector : zero and non-zero $\vec{k}$.

$$\langle C(\vec{k},t,t_0)\rangle_{ij} = \langle[\mathbf{Im}\sum_{\vec{x}} e^{i\vec{k}\cdot\vec{x}}P_{ij}(\vec{x},t)][\mathbf{Im}\sum_{\vec{x}} e^{-i\vec{k}\cdot\vec{x}}P_{ij}(\vec{x},t_0)]\rangle$$

Evaluation of the glueball correlator using the multi−level algorithm.

The thick black lines are held fixed during the sublattice averaging.

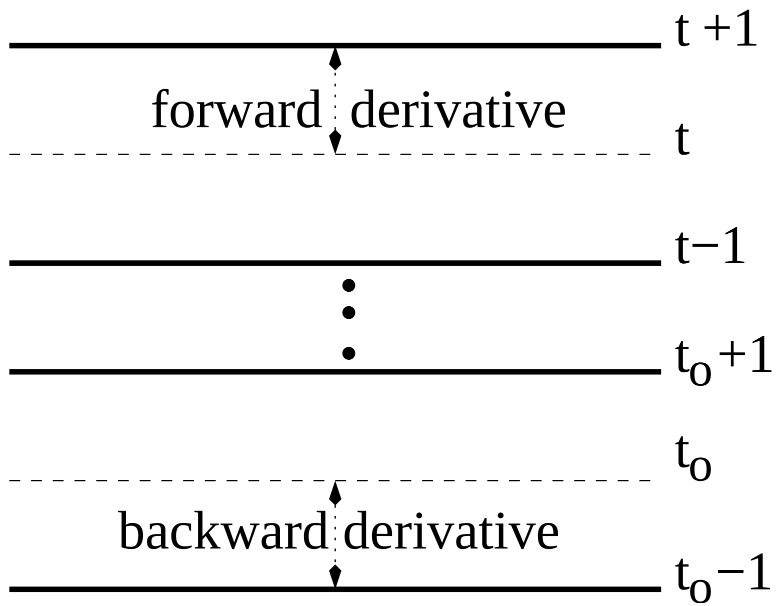

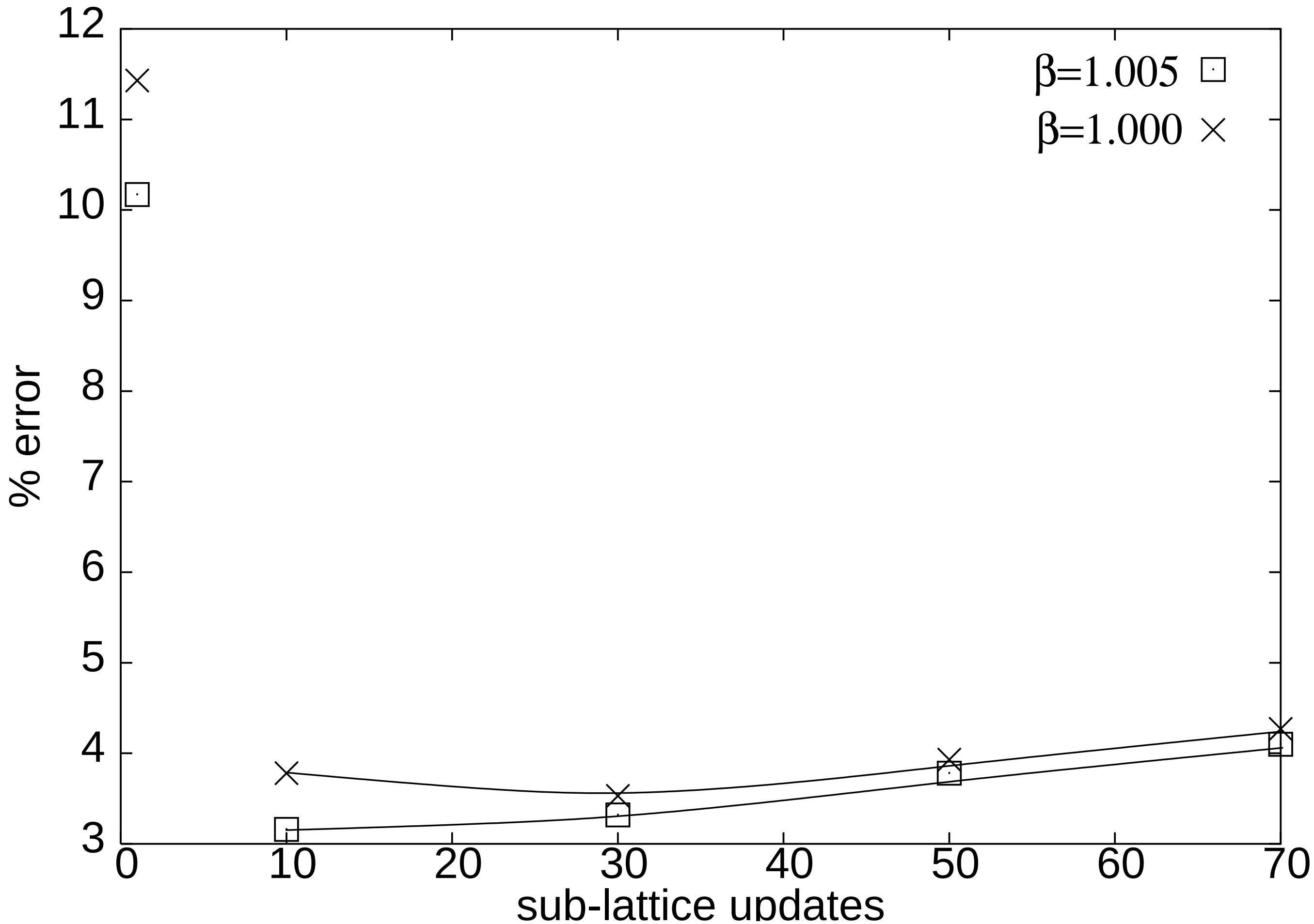

% Error on axial-vector correlator at $\Delta t = 2$ after a 10 hr run on a 1.5 GHz AMD Athlon PC. 12^4 lattice.

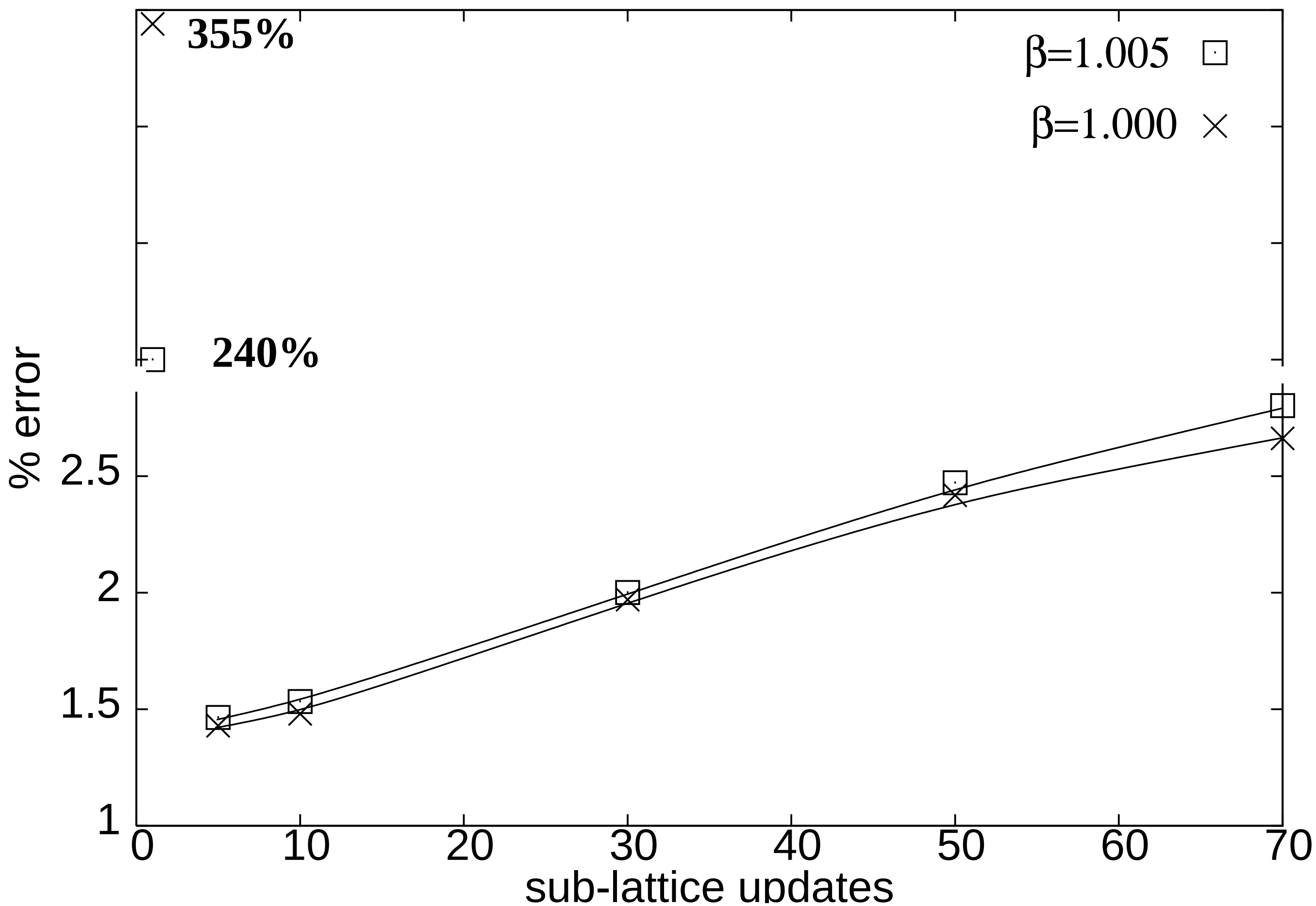

% Error on the scalar glueball correlator at $\Delta t = 2$ after a 10 hr run on a 1.5GHz AMD Athlon PC. 12^4 lattice.

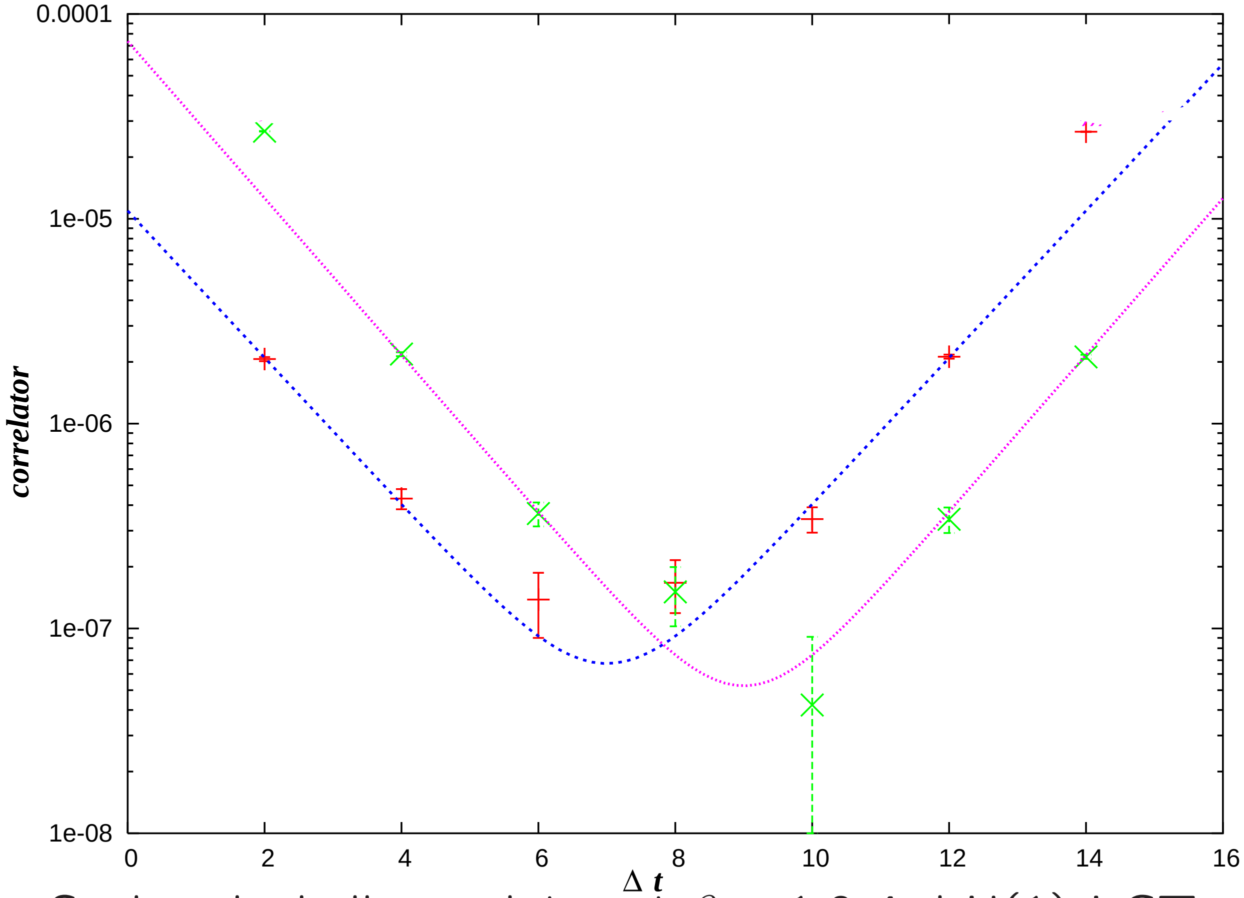

Scalar glueball correlator at $\beta = 1.0$ 4-d U(1) LGT

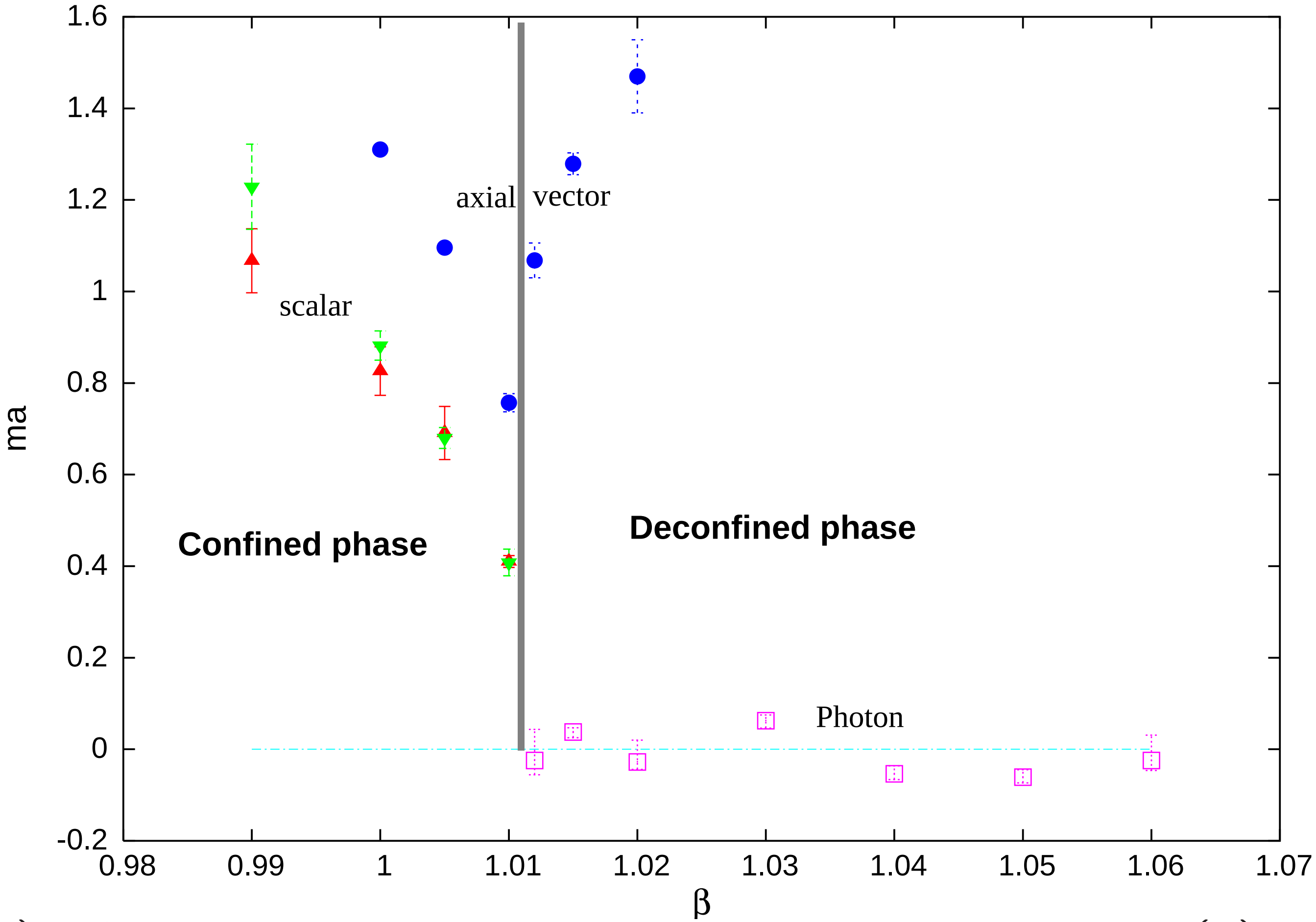

U(1) LGT scalar and axial vector glueball masses. 4-d U(1) LGT

Flux tube profile

- Distribution of electric field in flux tube
  a) thickness of flux-tube
  b) parameters for effective theory (dual superconductivity)

- $\langle \mathcal{O} \rangle = \dfrac{\langle P^* P \mathcal{O} \rangle}{\langle P^* P \rangle} - \langle \mathcal{O} \rangle$
  eg: Electric Field : $\mathcal{O}_E(n) = i\bar{\theta}_{\mu\nu} = i(\theta_{\mu\nu} - 2\pi n_{\mu\nu}(n))$

$$[P^*PO] = \frac{1}{3N_s^3(N_t/2)} \sum_{m_s,\, i}$$

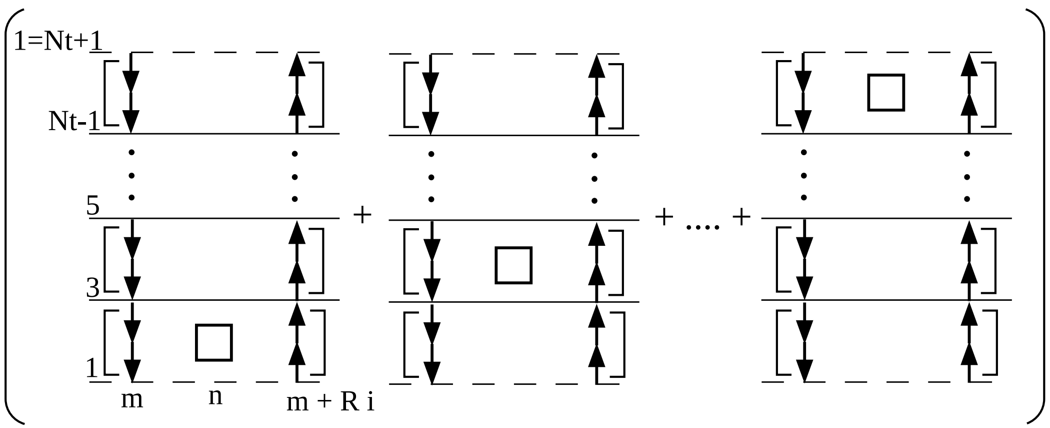

Conclusions

- We have seen how to achieve exponential error reduction in computation with pure Yang-Mills theories. The observables that people have looked at are
  - Ground state of the flux tube : M.Lüscher, P.Weisz
  - Excited states of the flux tube : P.Majumdar, Bastian Brandt
  - Profile of the flux tube : P.Majumdar, Y.Koma, M.Koma
  - Breaking of the flux tube : S.Kratochvila, Ph. de Forcrand
  - 3-quark potential : C.Alexandrou, Ph. de Forcrand, O. Jahn

- Glueball spectrum in SU(3) : H.B.Meyer
- Glueball spectrum in U(1) : P.Majumdar, Y.Koma, M.Koma

- The multilevel algorithm has to be applied in different ways for different observables. There is no single algorithm which works for everything. So one needs to think a bit before applying the algorithm.

Thank You